Chapter 2

Phase separation in a binary mixture of self-propelled particles with variable speed

2.1 Introduction

In the previous chapter.1, we have discussed the detail introduction of nonequilibrium statistical mechanics including historical background. The prototype Vicsek model includes that SPPs move with constant speed. However, in the real system SPPs move with different speed [Mishra et al. (2012)] and their collective behaviour is ubiquitous [Rauch et al. (1995)]. Examples range from very small intracellular scale to much larger scale [Ben-Jacob et al. (1995); Helbing et al. (2000); Hubbard et al. (2004); Kuusela et al. (2003); Marchetti et al. (2013a); Peruani et al. (2012); Ramaswamy (2010b); Rauch et al. (1995); Schaller et al. (2010); Sumino et al. (2012b); Surrey et al. (2001)]. Study of such systems started with the novel work of T. Vicsek [Vicsek et al. (1995)]. In Vicsek's study [Vicsek et al. (1995)], each individuals are modeled as point particle moving along their heading direction with a *constant* speed and align through a short range alignment interaction with

their neighbours. Interestingly different variants of Vicsek's model are studied but mainly with *constant* speed [Bhattacherjee et al. (2015); Chaté et al. (2006, 2007); Tunstrøm et al. (2013)]. But in natural systems, there is no reason for the speed of particles to be fixed. For examples in everyday traffic, a car can not move if stuck in a jam situation but moves freely, when other vehicles are moving in the same direction. Also in recent experiments on living bacteria *Bacillus Subtilis* by Luis *et al.*, it is observed that the speed of each individual (bacteria) depends on the local alignment of their neighbours [Cisneros et al. (2011)]. Similar behaviour is observed in experiments on fish school: motivated with such experiments, in previous study a variable speed model is introduced [Mishra et al. (2012)], such that speed of the particles depend on their local neighbours orientation through a variable speed parameter $\gamma > 0$ (with a *power*). For any $\gamma > 0$, when particle moves in a well-ordered region the speed is maximum and in the disordered region speed is close to zero. For $\gamma = 0$, all the particles move with *constant* speed. Hence model describes a system, where "random/ordered" crowd can "restrict/ease" the motion of the particle.
The power γ, a variable speed parameter is introduced which can be thought of as characteristics of particle, which implies how particle responds to its neighbours orientation. It can have origin from various biological or physical factors. In this chapter, we will not go into details of such factors. We will strictly consider a variable speed model introduced in [Mishra et al. (2012)] and ask the question what happens if we mix the particles with two different values of variable speed parameters (γ_1, γ_2)? Whether two types of particle can show phase separation for certain range of system parameters, *viz.* noise strength and γ?

In this chapter, we chose one of the $\gamma_1 = 1$ is fixed, *i.e.* speed of the particle linearly vary with local neighbours alignment. The other γ_2 is tuned from 0 to 8. The experiment on fish-school (Golden-Shiner) found that $\gamma = 6$ [Mishra et al. (2012)]. Hence some other kind of particles/species can have different γ.
Properties of the system are characterised by two types of order parameters (a) orientation

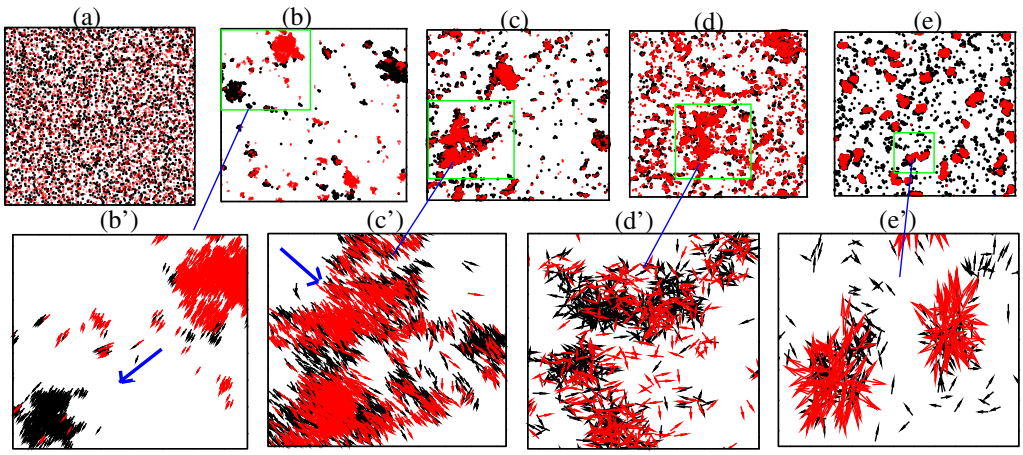

Fig. 2.1 (color online) Top panel: real space snapshots of position of two types of particles with the direction of their velocity vectors. Color represents two types of particles. Black is for particle of type one and red for second type particle. (a) is for initial random homogeneous mixed state, (b) is for ordered phase separated state ($\gamma_2 = 8$, $\eta = 0.2$), (c) ordered mixed ($\gamma_2 = 0.5$ $\eta = 0.2$, (d) is for disordered mixed ($\gamma_2 = 0.5$, $\eta = 0.62$) and (e) is for disordered phase segregated phase ($\gamma_2 = 8$, $\eta = 0.62$). (Bottom panel) (b'-e') are the zoomed version of top panel plot for better clarity of four different phases. All snapshots are collected in the steady state and plots are a part of the full system of size $L = 100$ or $N = 10^4$.

order parameter (OOP) χ, which is a measure of the global orientation of the flock and (b) density order parameter (DOP) ϕ, which is a measure of phase separation among two types of particles. We first measure the χ as a function of noise strength for different values of the variable speed parameter γ_2. For all set of γ's = (γ_1, γ_2) we find a transition from disordered-to-ordered state with the variation of noise strength, critical noise (is close to 0.6) is independent of the variable speed parameter γ. On the variation of two parameter (γ_2) and noise strength we find four distinct phases. (i) For small noise when system is globally ordered ($\chi \simeq 1$) and $\gamma_2 \geq 3$: the particles with two different γ's are phase separated and $\phi \simeq 1.0$. Hence they prefer to move in the group of their own type of particles. Typical snapshot for small $\eta = 0.2$ and $\gamma_2 = 8$ is shown in Fig. 2.1 (b) and (b'). This is named as ordered-phase separated (OPS). (ii) For small noise as γ_2 decreases the two types of particles form mixed moving clusters and hence ϕ decreases. This is defined as ordered mixed phase (OM). Please see the snapshot Fig. 2.1(c) and (c'). As we increase

noise strength and cross the ordered region $\eta > 0.6$, we again find two different phases (iii) disorder mixed (DM) and disordered phase segregated (DPS) when the difference in the two γ's is smaller/larger than 3. Please see the snapshot shown in Fig. 2.1(d,e) and (d',e').

In the rest of the chapter, we discuss the four distinct phases and also, compare the results with hydrodynamic equations of motion. Rest of the article is divided in the following manner. In section 2.2 we discuss the model and numerical details of the simulation. Section 2.3 contains the result of numerical study and in section 2.4 we compare the result with coarse-grained hydrodynamic equations of motion and finally section 2.6 concludes the result and discuss the final outcome of our study.

2.2 Model

We study a symmetric binary mixture of two types of self propelled particles with variable speed, moving on a two-dimensional substrate. Each particle is defined by its position $\mathbf{r}_i(t)$ and orientation angle $\theta_i(t)$. The velocity of the particle is defined by its unit direction $\mathbf{n}_i(t) = (\cos(\theta_i(t)), \sin(\theta_i(t))$ and *variable* speed $v_i(t)$. The particles interact through a short range alignment interaction. Unlike the previous models [Chaté et al. (2006); Vicsek et al. (1995)], here the speed of the particle depends on its neighbours, as given the variable speed model introduced in [Mishra et al. (2012)]. We first update the position of the particle

$$r_i(t+1) = r_i(t) + v_i(t)\mathbf{n_i}(t) \tag{2.1}$$

and the orientation update equation with a short range alignment interaction

$$\mathbf{n_i}(t+1) = \frac{\sum_{j\in R_0} \mathbf{n_j}(t) + N_i(t)\eta_i}{W_i(t)} \tag{2.2}$$

where the summation $\sum_{j\in R_0}$ is over all the particles within the interaction radius R_0 of the i^{th} particle, i.e., $|\mathbf{r}_j(t) - \mathbf{r}_i(t)| < R_0$. $N_i(t)$ is the number of particles within the interaction radius of the i^{th} particle at time t. $W_i(t)$ is the normalisation factor, which makes the R. H. S. of Eq $\sim$ 2.2 again a unit vector. The strength of the noise η is varied between 0 to 1. If $v_i(t) = v_0$ (constant), then the model is similar to Vicsek model [Vicsek et al. (1995)].

But unlike the Vicsek's model: we use a variable speed model as defined in [Mishra et al. (2012)] by considering a power-law relationship between the local polarisation $\chi_i(t)$ around i^{th} particle with speed $v_i(t)$ such that,

$$v_i(t) = v_0(\chi_i(t))^{\gamma} \tag{2.3}$$

where

$$\chi_i(t) = |\frac{\sum_{j\in R_0} \mathbf{n_j}(t)}{N_i(t)}| \tag{2.4}$$

and γ, is the variable speed parameter such that particle moves with maximum speed v_0 in well ordered region and almost static (zero speed) in completely disordered region. For $\gamma = 0$, model reduces to constant speed. Note that for any γ, an isolated particle will move with maximal speed v_0. Hence, the variable speed parameter γ controls the shape of curve that relates local order and speed.

In this chapter, we consider a symmetric binary mixture of particles by introducing two-types of particle parameters (two parameter γ_1 and γ_2) of speed such that $v_{i,1}(t) = v_0(\chi_i(t))^{\gamma_1}$ and $v_{i,2}(t) = v_0(\chi_i(t))^{\gamma_2}$. One of the γ, γ_1 is fixed to 1 and these particles are called as *type one* and other γ_2 is varied from 0 to 8 and these particles are called *type two*. Agent based numerical simulation is performed with N_1 particles of type one and N_2 particles of type two ($N_1 = N_2 = N/2$), where N is the total number of particles on a two dimensional lattice of size $L \times L$ with periodic boundary condition. Started with random mixed state of both types of particles, all the particles are sequentially updated using the

above Eqs $\sim$ 2.1,2.2,2.3,2.4 and it is counted as one simulation step. Simulations are performed for 10^7 simulation steps with $L = 100, 200$ (N=$10^4, 4\times10^4$). The density of particle is fixed to $\rho = \frac{N}{L^2} = 1.0$ and the maximum speed of the particle $v_0 = 0.5$. For better quality of data, five different initial realisations are used. We study the system for different sets of (γ_2, η). Steady state is characterised by two types of order parameters: (i) orientation order parameter (*OOP*) $\chi(t) = |\frac{1}{N}\sum_{i=1}^{N} \mathbf{n}_i(t)|$, which is a measure of orientation of all the particles. For $\chi(t) \simeq 1$ (ordered state), large number of particles moving in the same direction, showing the collective motion. If $\chi(t) = 0$ i.e. all the particles moving in random directions (disorder state). (ii) Density order parameter (*DOP*) $\phi = \frac{\sum_{i=1}^{N} |\rho_1^i(t) - \rho_2^i(t)|}{\sum_{i=1}^{N} |\rho_1^i(t) + \rho_2^i(t)|}$, which is a measure of phase separation among two types of particles, where $\rho^i_{k=1,2}(t)$ are the number of particle of type k within the coarse-grained radius of i^{th} particle of same type. The value of ϕ also lies between 0 and 1. When ϕ close to 1, implies only the same kind of particle inside the interaction radius, which implies phase separation. When ϕ is small, both types of particles present in same proportion inside the interaction radius hence mixing.

2.3 Results

We first calculate the "mean" value of *OOP* χ, averaged over time in the steady state and over 10 realisations. In Fig. 2.2 we plot the steady state χ vs. η for different $\gamma_2 = 0.5, 2, 4, 6$. For all set of γ_2, we find a transition from disordered random state to ordered state when η is tuned from 1 to 0. It is observed that for all γ_2, transition remains the same. Hence disorder-to-order transition is independent of the variable speed parameter γ. We also calculate the *mean* value of *DOP* ϕ, where the definition of "mean" is same as defined earlier. We find four distinct phases on varying system parameters (η, γ_2). (a) Ordered phase separated (OPS), (b) ordered mixed (OM), (c) disordered mixed (DM) and (d) disordered phase segregated (DPS). In Fig. 2.1 we plot the four snapshots for four

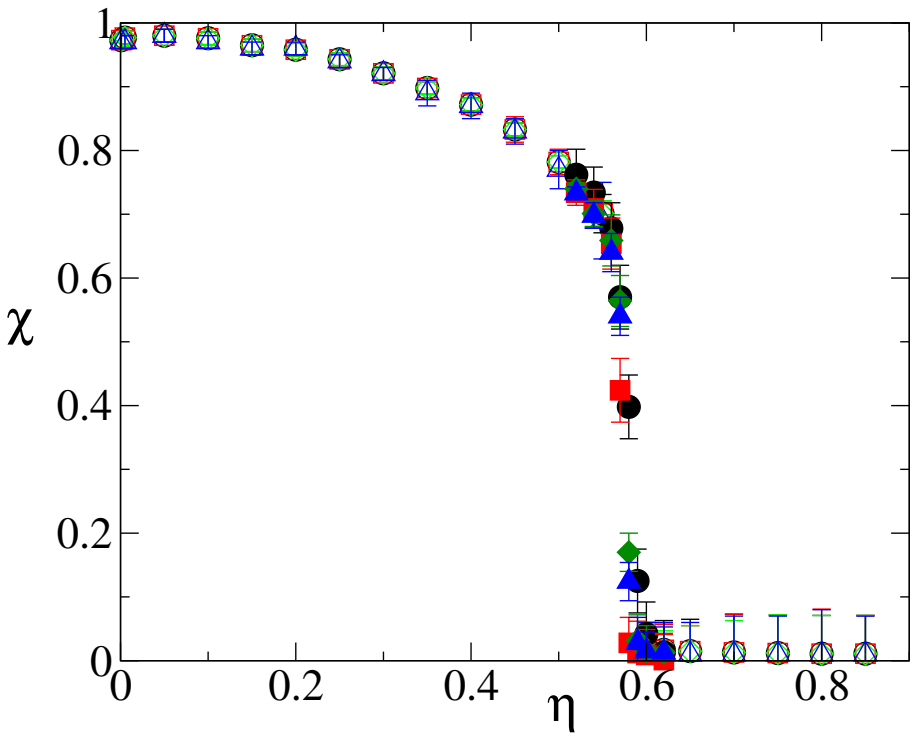

Fig. 2.2 (color online) Plot of orientation order parameter (OOP) vs. noise strength η, $\gamma_1 = 1$, different curves are for different γ_2. $\circ$, $\square$, $\diamond$ and $\triangle$ are for $\gamma_2 = 0.5, 2, 4$ and 6 respectively. Empty symbols denote data for $L = 100$, or $N = 10^4$ and filled ones are for $L = 200$ or $N = 4 \times 10^4$. For $L = 200$ more number of data points are obtained near order-to-disorder phase transition. For all γ_2, critical noise lies between $0.57 - 0.60$. Total simulation time is 10^7 and data is extracted from last 10^6 times in the steady state. Averaging is done over five independent realisations.

combination of (γ_2, η). Since for all γ_2 disorder-to-order transition happens at same η, hence all of our later measurements are strictly restricted to *ordered* state ($\eta < 0.4$) and *disordered* state ($\eta > 0.6$). Properties near to the disorder-to-order transition are also interesting but it is not of our interest in this chapter.

For small $\eta = 0.2$ and larger $\gamma_2 > 3$, we find *OOP*, $\chi \simeq 1$ and also $\phi \simeq 1$, hence in the steady state particles form ordered clusters and also phase separate. Typical snapshot for this kind of phase is shown in Fig. 2.1(b) and (b'). We name it as order phase separated (OPS). As we decrease the γ_2 then the difference in the speed of two types of particle decreases and they start to mix. Fig. 2.1(c) and (c') show one of the typical snapshots of such phase. We call such phase as order mixed (OM). In this phase χ, is still close to 1

but $\phi < 0.6$. Now as we go to the disordered state $\eta > 0.6$ and vary γ_2. For small $\gamma_2 < 3$, the two types of particles are always mixed. Both ϕ and χ are small, we call this phase as disorder mixed (DM) and for large $\gamma_2 > 3$, we find disorder-phase segregated phase (DPS), where ϕ approaches moderate values but the two phases differ in detail, which we will explain in the following subsections. Typical snapshots of the two phases are shown in Fig.2.1 (d-e) and (d'-e') respectively.

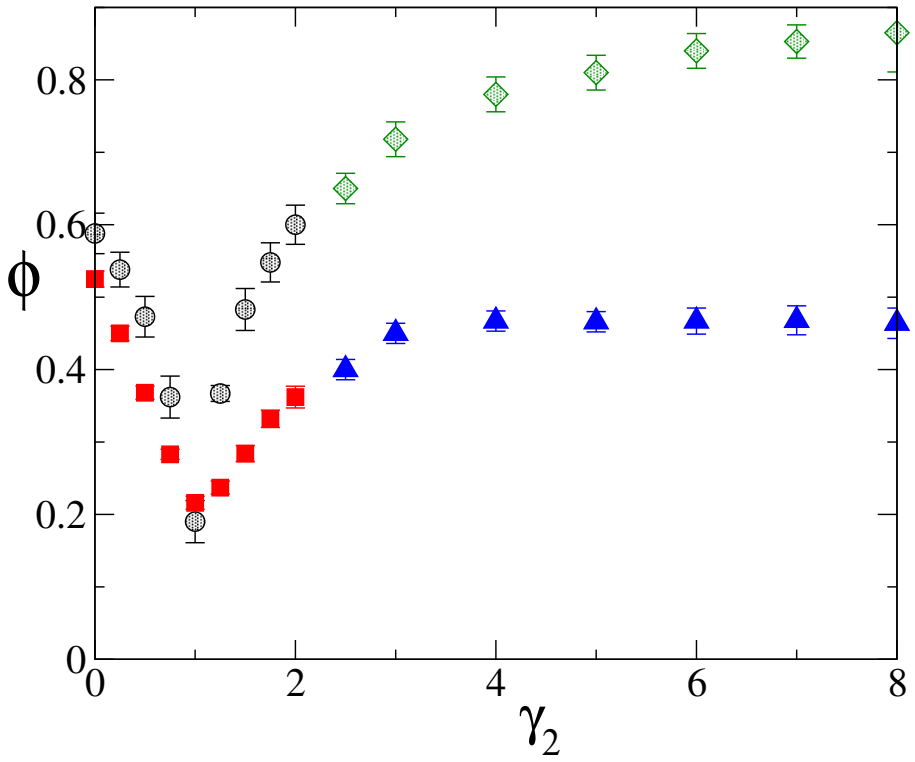

Fig. 2.3 (color online): Plot of DOP vs. γ_2 for two different $\eta = 0.2$ (*partially filled*) and 0.62 (*filled*). Other parameters are same as defined in Fig. 2.1. Different symbols denote the four different phases in the system (i) Green diamond represents OPS for $(2 < \gamma_2)$. (ii) Black circle shows OM phase $(0 < \gamma_2 < 2)$. (iii) Red square represents DM phase for $0 < \gamma_2 < 2$ and (iv) Blue triangles for DPS phase for $(2 < \gamma_2)$.

2.3.1 Ordered Phase Separated: OPS

For small η and large γ_2, the two order parameters *OOP* and *DOP* are close to 1. In Fig.2.3 we plot the *DOP* vs. γ_2 for two different $\eta = (0.2, 0.62)$ values. For small $\eta = 0.2$, starting from an initial random and mixed state at late time, both types of particles form moving clusters, but they move in clusters of their own type of particles. For larger γ_2 and smaller η, clusters are more separated and as we increase η and decrease γ_2, phase separation decreases as shown in Fig. 2.3. To further understand the behaviour, we calculate the probability distribution function (PDF) of speed $P(v)$ for two types of particles. In Fig.2.4(a) we plot the $P(v)$ for both types of the particle for two different $\gamma_2 = 8$ and $\gamma_1 = 1$ and for noise strength $\eta = 0.2$. For both types of particle we find one small peak at maximum possible speed $v = 0.5$, which is mainly due to the random moving particles. Another peak is present at a smaller speed value $v < 0.5$. This is the contribution from the clusters. Smaller peak fits well with Gaussian distribution (lines are fit to the Gaussian distribution). We find that the difference in the two peak positions $\Delta V/v_0$ increases as we increase γ_2. Peak position represents the mean speed of moving clusters. In Fig. 2.6 we plot $\Delta V/v_0$ vs. γ_2 for $\eta = 0.2$.

In section 2.4 we show the linearised study of coarse-grained hydrodynamic equations of motion for the density of two types of particles and polarisation order parameter. The equations are studied for small fluctuations about the homogeneous ordered state for different value of γ_2. We find that homogeneous ordered state is unstable for large γ_2 and η. Which confirms the presence of *OPS* phase for large γ_2 and small η. To further characterise different phases we calculate the PDF of number of particles in the interaction radius $P_{ij}(n)$, where $(i, j = 1, 2)$ and n is number of particles of j-type in the interaction radius of particle of type i. In this phase, the two distributions $P_{12}(n)$ and $P_{21}(n)$ look similar, and show sharp decay at larger n, which is due to small probability of mixing of two types of particles. Other two distributions $P_{11}(n)$ and $P_{22}(n)$ have broad distribution

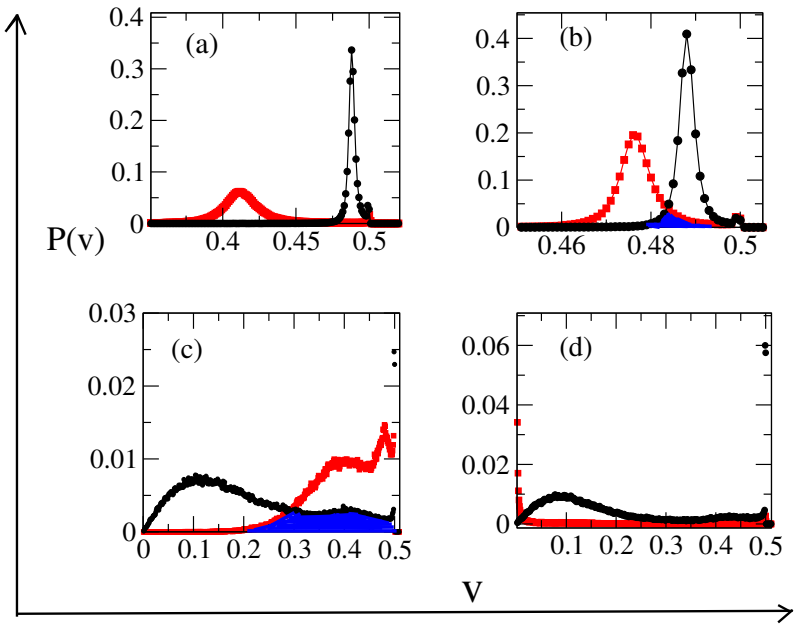

Fig. 2.4 Plot of PDF of speed $P(v)$ vs. v for four different phases (a-d) for OPS, OM, DM and DPS respectively. The two curves are for $P(v)$ for two types of particles. $\circ$ and $\square$ is for the particle of type one and two respectively. For all plots, there is always a peak at maximum speed $v = v_0 = 0.5$ and second peak is at smaller v value. The difference in two peak positions is large for large γ_2 in the ordered state. The shaded area ((b) and (c)) show the extent of mixing of particles of type one and two. Other parameters are same as in Fig.2.2 and $N = 10^4$

which confirms the clustering of same type of particles. Please see the Fig. 2.5(a). In the lower panel of Fig. 2.5(a) we plot the $P_{ij}(n)$ on $\log - \log$ scale. It shows that the tail of $P_{12}(n)$ and $P_{21}(n)$ fits well with power $n^{-\alpha}$ with exponent $\alpha \simeq 2$, but $P_{11}(n)$ and $P_{22}(n)$ are better fitted with $exp(\frac{-n}{n_0})$ and $n_0 \simeq 40$, where n_0 can be approximated as mean number of particles in the interaction radius.

2.3.2 Ordered Mixed: OM

In this phase as defined before orientation of particles are aligned along some mean direction and hence *OOP* is close to 1, but both types of particles remain mix and a cluster consists of both types of particles as shown in Fig. 2.1(c) and (c'), hence small *DOP*. In Fig. 2.4(b) we plot the $P(v)$ for $\gamma_2 = 0.5$ and $\eta = 0.2$. We notice two features in the

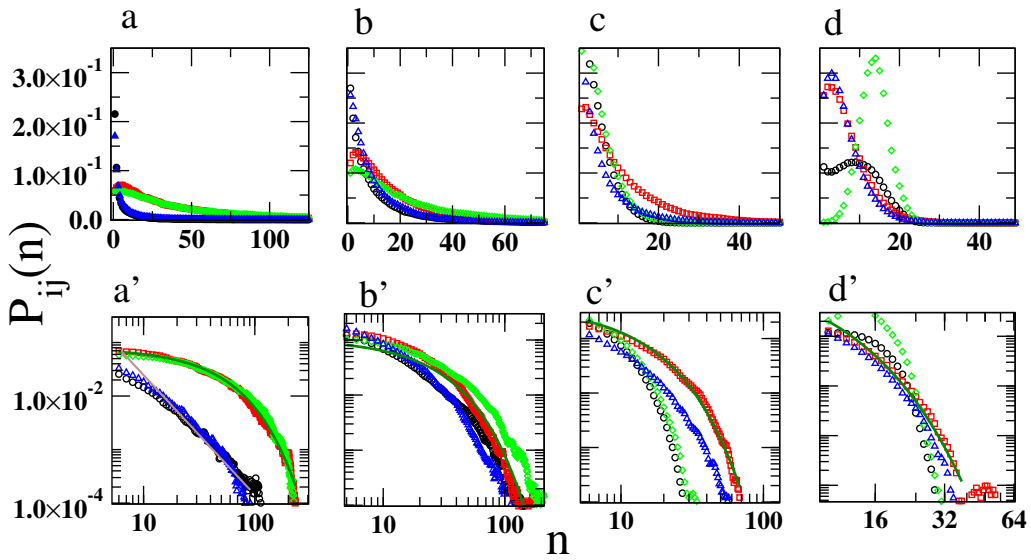

Fig. 2.5 (color online): Plot of particle number PDF, $P_{ij}(n)$ for four different phases OPS, OM, DM and DPS, (a-d) respectively. Top panel is plot on normal scale and bottom is on log-log scale. The four curves in each panel are for four distributions as defined in the main text. $\circ$, $\square$, $\diamond$ and $\triangle$'s are for $P_{12}(n)$, $P_{11}(n)$, $P_{22}(n)$ and $P_{21}(n)$ respectively. In the bottom panel curves are fitted with power-law and exponential tail for large n. Other parameters are same as in Fig. 2.1

$P(v)$, one peak at $v = 0.5$ which is again due to the random isolated moving particles. The second peak appears at $v < 0.5$ for both types of particle. In comparison to the previous case, now the difference in the two peak position decreases and the two distributions start to overlap as shown in Fig. 2.4(b). The overlap between the distributions is due to a large number of both types particles moving with the same speed. Hence they belong to the same cluster. Again we plot the the four $P_{ij}(n)$ in Fig. 2.5, all four $P_{ij}(n)$ decay exponentially with $n_0 \approx 20-30$, which implies formation of large clusters. But all four distributions are similar, hence one type of particle can be in the neighborhood of other type and also of the same type with equal probability. Which again confirms the mixed phase.

2.3.3 Disordered Mixed: DM

Now we come to the case when noise strength is large such that mean orientation of particle is random but difference in two types of γ is small, $\gamma_2 < 3$. In this case both order

parameters remain small. Hence we name the phase as disordered mixed phase. First the four number distributions $P_{ij}(n)$ are exponential with $n_0 \simeq 3$ for $P_{11}(n)$ and $n_0 \simeq 8$ for $P_{12}(n)$ and approximately close to 10 for $P_{22}(n)$ and $P_{21}(n)$. Size of clusters are small in this phase and particles of type one form even smaller clusters. $P(v)$ shows broad distribution for both types of particles and with very clear overlap. Which further confirms the mixing.

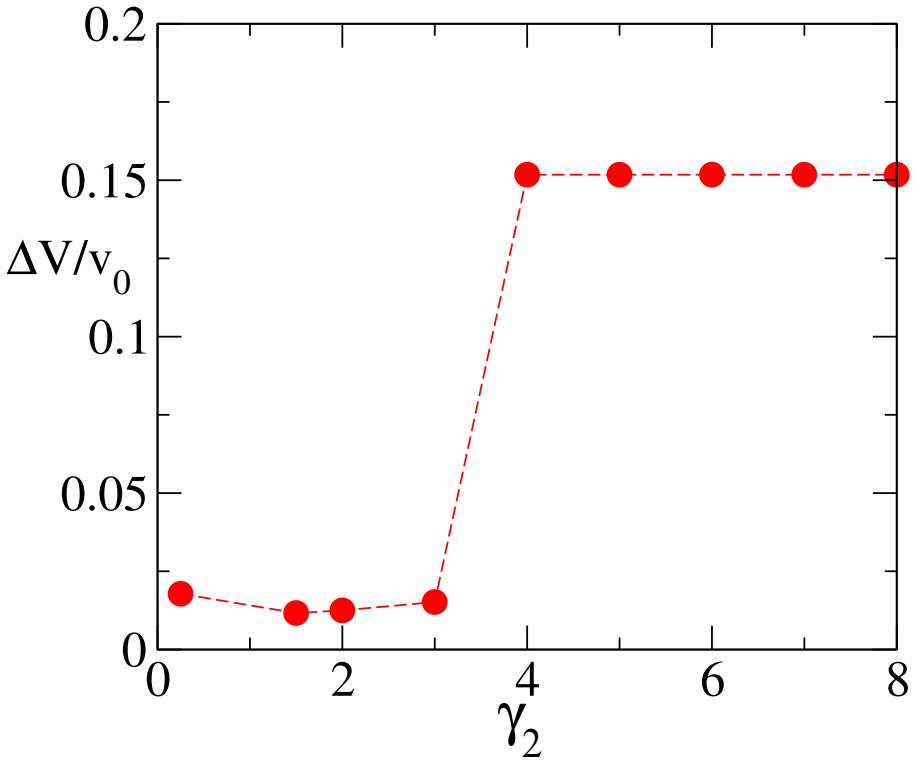

Fig. 2.6 Plot of normalised velocity difference $\Delta V/v_0$ vs. γ_2 for the ordered state $\eta = 0.2$. Other parameters are same as in Fig. 2.1

2.3.4 Disordered Phase Segregated: DPS

When noise is large $\eta > 0.6$ and we tune γ_2. For large $\gamma_2 > 3$, i.e. for type one $\gamma_1 = 1$ particle speed varies linearly with local polarisation. For the second type $\gamma_2 >> \gamma_1$, hence speed is close to maximum speed for well-ordered regions and very small for disordered region. Remember in the disordered region when $\eta > 0.6$, most of the time particles are in

disordered cluster region or moving individually. For type one particle, since speed varies linearly with local polarisation hence we find a broad distribution of $P(v)$ and another type particle, speed can mainly take two possible values v_0 and 0 when a particle is isolated or in cluster respectively. In Fig. 2.1(e) and (e') we plot the real space snapshot of particle position for both types of particles. We find that one type of particles, for which γ is large > 4, particles form static clusters shown in red and another type of particles are part of the static cluster partially and partially they are moving randomly (as shown in black arrow in Fig. 2.1(e)) . In the bottom panel, we show the zoomed version of the same snapshot for a small part of the total system. It shows that orientation of particles inside the cluster is random. In Fig. 2.4 we plot $P(v)$, which shows a broad distribution for type one particles and two distinct peaks at $v = 0.5$ and $v = 0.0$ for type two particles (Which again due to static clusters). Size of the peak at $v = 0.5$ is large for type one particle in comparison to the second type. Hence a large number of type one particles are moving randomly. To further characterise this phase also plot the four $P_{ij}(n)$'s. In this case, the four distributions are very different from the previous cases. We find that $P_{11}(n)$ is Gaussian and shows a peak at some finite value of n. That typically represents the mean number of particles in the interaction radius. This is due to the presence of type one particle in the static regions of the cluster formed by second type particles, which acts like nucleation site for the particles of type one. The $P_{12}(n)$, shows a broad distribution which confirms that the cluster of particle of type one has another particle too (due to fixed second type particle). The two other distributions $P_{22}(n)$ and $P_{21}(n)$ are similar. When plotted on $\log - \log$ scale, the two P_{21} and P_{22} shows exponential tail with $n_0 \approx 5$.

2.3.5 Dynamics of particle in DM and DPS phase

We also characterise the dynamics of both types of particles in DM and DPS phase. We first calculate the mean square displacement MSD, $\Delta_i(t) =< |\mathbf{r}_i(t+t_0) - \mathbf{r}_i(t)|^2 >$, where

$i = 1,2$ for particle of type one and two respectively. $< . >$ is average over all the particles of same type and many reference time t_0. MSD is calculated for $\eta = 0.62$ and for different γ_2. In the disordered region or when $\eta > 0.6$ we find that for both $\Delta_i(t) \simeq t$, which suggest the diffusive behavior of particles. We further estimate the effective diffusion coefficient $D_{eff} = \lim_{t\to\infty} \frac{\Delta(t)}{4t}$. Hence in Fig. 2.7 we plot the effective diffusion coefficient D_{eff} vs. γ_2. For small γ_2, diffusivity of both types of particle is finite but as we increase γ_2, diffusivity of second type particle is almost zero. Which suggest static clusters of second type particle as found in DPS phase. Whereas diffusivity of type one particle remains constant on varying γ_2.

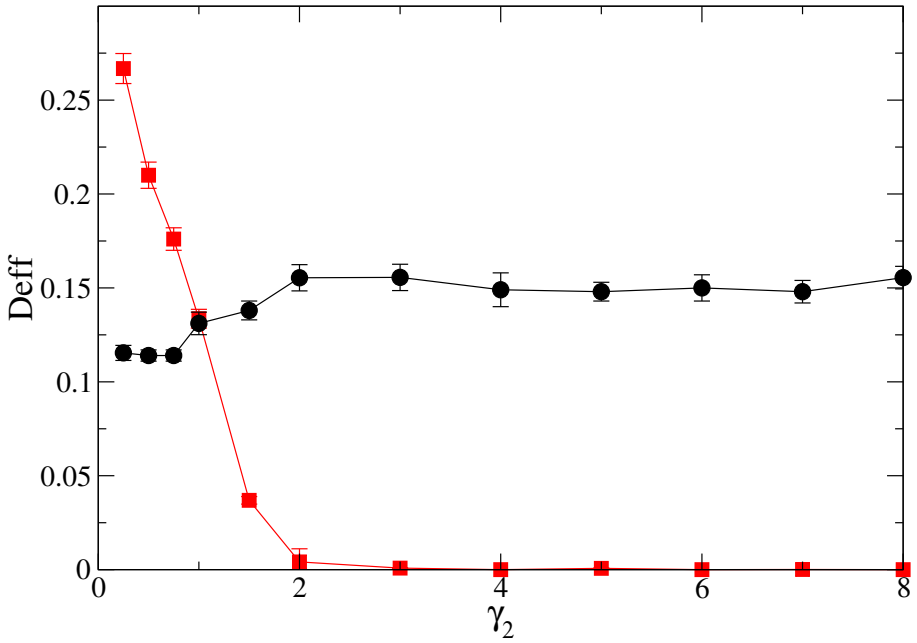

Fig. 2.7 Plot of effective diffusivity D_{eff} vs. γ_2 in the disordered region $\eta = 0.65$ for two types of particles. ○, □ is for particle of type one and two respectively. Other parameters are same as given in Fig. 2.1

2.4 Coarse-grained hydrodynamics

In this section we will discuss the presence of OPS state for large γ_2 and in the ordered state $\eta < 0.6$ using the coarse-grained hydrodynamic equations of motion for slow or

hydrodynamic variables. For our model, relevant hydrodynamic variables are coarse-grained (i) density $\rho_1(\mathbf{r},t)$ of types one and $\rho_2(\mathbf{r},t)$ of type two particle because total density of both types of particles are fixed and (ii) polarisation order parameter $\mathbf{P}(\mathbf{r},t)$ because it is a broken symmetry variable in the aligned (ordered) state. First we write the equation for density of both types particles

$$\partial_t \rho_1 = -\nabla\cdot(v_1\mathbf{P}\rho_1) + \frac{1}{2}D\nabla^2({v_1}^2\rho_1) \tag{2.5}$$

$$\partial_t \rho_2 = -\nabla\cdot(v_2\mathbf{P}\rho_2) + \frac{1}{2}D\nabla^2(v_2^2\rho_2) \tag{2.6}$$

where v_i $(i=1,2)$ is self-propulsion speed of particle of type one and two respectively. In the variable speed model, it depends on the local polarisation $\mathbf{P}(\mathbf{r},t)$ and variable speed parameter γ_i. The above equations 2.5, 2.6 are the continuity equation $\partial_t\rho_i = -\nabla\cdot\mathbf{J}_i$ $(i=1,2)$. The current $\mathbf{J}_i$ contains two types of terms. The first term is due to the active nature of particles. The active current $\mathbf{J}_{i,a}$, is proportional to the local velocity $v_i\mathbf{P}$ of particle of type i. Second term in both equations is due to diffusive current. For simplicity we choose the same diffusion coefficient D for both types of particles. Now we come to the equation for the polarisation order parameter $\mathbf{P}(\mathbf{r},t)$. Following the coarse-grained approach as in [Bertin et al. (2013); Bhattacherjee et al. (2015); Mishra et al. (2012); Toner & Tu (1995)], the polarisation equation will have following leading order terms

$$\begin{aligned}\partial_t\mathbf{P} &= \big(\alpha_1(\rho,\eta) - \alpha_2\mathbf{P}\cdot\mathbf{P}\big)\mathbf{P} - \frac{1}{2}\nabla(v_1\rho_1) \\ &\quad -\frac{1}{2}\nabla(v_2\rho_2) + \lambda(\mathbf{P}\cdot\nabla)\mathbf{P} + k\nabla^2\mathbf{P}\end{aligned} \tag{2.7}$$

where on the R. H. S. of above equation the first term is the polynomial term which determines the disorder-to-order mean field transition. The second and third terms, the two gradients in density, is the change in local polarisation due to the variation in density of two types of particles, λ term is the non-linear term and coefficient λ in general depends on the microscopic parameters *viz* (mean density ρ_0, speed v_0 etc.). In general we have three kinds of non-linearities as given in [Bertin et al. (2013); Bhattacherjee et al. (2015); Mishra et al. (2012); Toner & Tu (1995)] but we keep only one of the relevant one as shown in recent study of [Toner & Tu (1995)]. The last term is the diffusion of local polarisation. Hence the three equations 2.5, 2.6 and 2.7 describes the coarse-grained decription of model defined in Eqs $\sim$ 2.1, 2.2, 2.3 and 2.4.

The homogeneous-ordered steady state solution of above equations are $\rho_1 = \rho_2 = \rho_0/2$ and polarisation $\mathbf{P} = P_0\hat{x} + 0\hat{y}$, where $P_0 = \sqrt{\frac{\alpha_1(\rho_0)}{\alpha_2}}$ is obtained from homogeneous steady state solution of Eq $\sim$2.7. Now we discuss the stability analysis of these equations with respect to homogeneous ordered state. When purturbed from such homogeneous state and write linear equations for small fluctuations in local density and polaristaion $(\delta\rho_1, \delta\rho_2, \delta P_{||}, \delta P_{\perp})$ Where $\delta P_{||}$ and $\delta P_{\perp}$ are two components of small fluctuations in the direction and perpendicular to the mean polarisation. Deep in the ordered state hence small $\delta P_{||}$, and solving for $\delta P_{||}$ we find a coupled equation for two density fluctuations and $\delta P_{\perp}$. Detail calculation of linearised hydrodynamic equations is given in section.2.5. In the longitudinal direction one of mode decoupled and we find two coupled modes with the following structure from Eq $\sim$2.26 in the section.2.5

$$S_- = -[v_1 p_0 iq + D_+ q^2] \tag{2.8}$$

and

$$S_+ = -[v_2 p_0 iq + D_- q^2] \tag{2.9}$$

clearly $\mathscr{R}](S)$ determines the stability of mode, one of the mode S_- which is always statble and other mode S_+ can become unstable if $D_- < 0 \Rightarrow \Delta v > \frac{4D\alpha_1}{v_2\rho_{10}} \Rightarrow (\frac{8D\alpha_1}{v_2\rho_0})$ where $\Delta v = v_1 - v_2$ and since $v_2 = v_0 {p_0}^{\gamma_2}$ and $p_0 < 1$ hence for large γ_2, v_2 becomes smaller and smaller hence more stable solution as found in simulation. The above condition satisfies for large difference in two $\gamma' s$ and larger P_0 (smaller η). Similar feature is obtained in our numerical simulation when for large γ and small η the two types of particles move in different clusters in ordered phase seprated phase as shown in Fig. 2.3.

2.5 Linearised study of hydrodynamic equations of motion

Now we use the hydrodynamics Eqs $\sim$ 2.5, 2.6 and 2.7 and write the linear equations for small fluctuations about the homogeneous ordered mixed state. Using the mean-field approximation, the speed of two types of particles can be replaced by $v_{1,2} = v_0 {p_0}^{\gamma_1,\gamma_2}$, where $p_0 = \sqrt{\frac{\alpha_1(\rho_0)}{\alpha_2}}$ from Eq $\sim$2.7. Using the two density equations we write the equation in terms of difference in the density of both types of particles $\Delta\rho = \rho_1 - \rho_2$

$$\partial_t \Delta\rho = -v_1 \nabla \cdot (\mathbf{P}\rho_1) + v_2 \nabla \cdot (\mathbf{P}\rho_2) + D\nabla^2 \Delta\rho \tag{2.10}$$

which is further equal to

$$\partial_t \Delta\rho = -\Delta v \nabla \cdot (\mathbf{P}\rho_1) - v_2 \nabla \cdot (\mathbf{P}\Delta\rho) + D\nabla^2 \Delta\rho \tag{2.11}$$

where $\Delta v = v_1 - v_2$ is the difference in two mean field speed and equation for the density of particle of type one is same as in Eq $\sim$ 2.5. In the same manner we write the polarisation

equation also in terms of $\Delta\rho$ and Δv

$$\begin{aligned}\partial_t \mathbf{P} &= \big(\alpha_1(\rho,\eta) - \alpha_2 \mathbf{P}\cdot\mathbf{P}\big)\mathbf{P} - \frac{\overline{v}}{2}\nabla(\rho_1) + \frac{v_1}{2}\nabla(\Delta\rho) \\ &\quad -\frac{\Delta v}{2}\nabla(\Delta\rho) + \lambda(\mathbf{P}\cdot\nabla)\mathbf{P} + k\nabla^2\mathbf{P} + \mathbf{H} \end{aligned} \tag{2.12}$$

Where, $\overline{v} = v_1 + v_2$. The homogeneous steady state solution of above three equations for $\Delta\rho$, ρ_1 and $\mathbf{P}$ is $\Delta\rho = 0$, $\rho_1 = 0$ and $\mathbf{P} = \sqrt{\frac{\alpha_1}{\alpha_2}}\widehat{\mathbf{x}}$ (the direction of broken symmetry along $x-$axis). We add small perturbation about the above homogeneous solution and replace $\Delta\rho(\mathbf{r},t) = \delta\Delta\rho$, $\rho_1(\mathbf{r},t) = \rho_{10} + \delta\rho_1$ and $\mathbf{P}(\mathbf{r},t) = (p_0 + \delta p_\parallel)\widehat{\mathbf{x}} + (\delta p_\perp)\widehat{\mathbf{y}}$, where $p_0 = \sqrt{\frac{\alpha_1}{\alpha_2}}$ and $\delta\Delta\rho = \delta\rho_1 - \delta\rho_2$ is the fluctuation in the two densities about their mean values. In later part, for simplicity we write $\delta\Delta\rho = \Delta\rho$. Now we write the equations for small perturbations in four fields $\Delta\rho$, $\delta\rho_1$, $\delta p_\parallel$ and $\delta p_\perp$. We first write the equation for $\delta p_\parallel$

$$\begin{aligned}\partial_t \delta p_\parallel &= \big(\alpha_1(\rho_0) - \alpha_2(p_0^2 + 2p_0\delta p_\parallel)\big)(p_0 + \delta p_\parallel) - \frac{v_1}{2}\nabla\delta\rho_1 \\ &\quad -\frac{v_2}{2}\nabla(\rho_1 - \Delta\rho) + \lambda(p_0\partial_x)\delta p_\parallel + k\nabla^2\delta p_\parallel \end{aligned} \tag{2.13}$$

Ignoring the higher order gradient terms and in the steady state

$$\delta p_\parallel(\mathbf{r},t) = -\frac{1}{4\alpha_1}(v_1 + v_2)\partial_x\delta\rho_1 + \frac{v_2}{4\alpha_1}\partial_x(\Delta\rho) \tag{2.14}$$

Now we write the equations for the small fluctuations in other three field and substitute the expression for $\delta p_\parallel$ from Eq $\sim$ 2.11

$$\partial_t \delta p_\perp = -\frac{v_1}{2}\partial_y\delta\rho_1 - \frac{v_2}{2}\partial_y(\delta\rho_1 - \Delta\rho) + \lambda(p_0\partial_x)\delta p_\perp + k\nabla^2\delta p_\perp \tag{2.15}$$

The new equation for $\delta\rho_1$ and $\delta\Delta\rho$ are obtained by substituting solution of $\delta p_{\|}$ from equation 2.12 in equation 2.5 and 2.6,

$$\partial_t \delta\rho_1 = -v_1 p_0 \partial_x \delta\rho_1 + \frac{\bar{v} v_1 \rho_{10} \partial_x{}^2 \delta\rho_1}{4\alpha_1} - \frac{v_1 v_2 \rho_{10} \partial_x{}^2 \Delta\rho}{4\alpha_1} - v_1 \rho_{10} \partial_y \delta p_\perp + D\nabla^2 \delta\rho_1 \tag{2.16}$$

$$\partial_t \Delta\rho = -\Delta v p_0 \partial_x \delta\rho_1 + \frac{\bar{v} \Delta v \rho_{10} \partial_x^2 \delta\rho_1}{4\alpha_1} - \frac{v_2 \Delta v \rho_{10} \partial_x^2 \Delta\rho}{4\alpha_1} - \Delta v \rho_{10} \partial_y \delta p_\perp - v_2 p_0 \partial_x \Delta\rho + D\nabla^2 \Delta\rho \tag{2.17}$$

now taking the Fourier transformation equation 2.15 2.16 and 2.17 by using

$$Y = \begin{bmatrix} \delta\rho_1 \\ \Delta\rho \\ \delta p_\perp \end{bmatrix}, Y(k,S) = \int Y(r,t) \exp(St - i\bar{k}\cdot\bar{r}) d\bar{r} dt \tag{2.18}$$

and write in Fourier space

$$(S + v_1 p_0 i q_x + \frac{\bar{v} v_1 \rho_{10} q_x^2}{4\alpha_1} + Dq^2)\delta\rho_1 - (\frac{v_1 v_2 \rho_{10} q_x^2}{4\alpha_1})\Delta\rho + v_1 \rho_{10} i q_y \delta p_\perp = 0 \tag{2.19}$$

$$(\Delta v p_0 i q_x + \frac{\Delta v \bar{v} \rho_{10} q_x^2}{4\alpha_1})\delta\rho_1 + (S - \frac{\Delta v v_2 \rho_{10} q_x^2}{4\alpha_1} + Dq^2 + v_2 p_0 i q_x)\Delta\rho + \Delta v \rho_{10} i q_y \delta p_\perp = 0 \tag{2.20}$$

$$(\frac{v_1 i q_y}{2} + \frac{v_2 i q_y}{2})\delta\rho_1 - (\frac{v_2 i q_y}{2})\Delta\rho + (S - \lambda p_0 i q_x + k q^2)\Delta p_\perp = 0 \tag{2.21}$$

$M \times Y = 0$ where

$$M = \begin{bmatrix} (S + v_1 p_0 i q_x + \frac{\bar{v} v_1 \rho_{10} q_x^2}{4\alpha_1} + Dq^2) & (-v_1 v_2 \rho_{10} q_x^2 / 4\alpha_1) & (v_1 \rho_{10} i q_y) \\ (\Delta v p_0 i q_x + \frac{\Delta v \bar{v} \rho_{10} q_x^2}{4\alpha_1}) & (S - \frac{\Delta v v_2 \rho_{10} q_x^2}{4\alpha_1} + Dq^2 + v_2 p_0 i q_x) & (\Delta v \rho_{10} i q_y) \\ (\frac{\bar{v}}{2} i q_y) & (-\frac{v_2}{2} i q_y) & (S - \lambda p_0 i q_x + k q^2) \end{bmatrix} \begin{bmatrix} \delta\rho_1 \\ \Delta\rho \\ \delta p_\perp \end{bmatrix} \tag{2.22}$$

Now we focus along the ordering direction $q_y = 0, \theta = 0, q_x = q$ and $det[M] = 0$

Eq ∼2.22 can be solved for modes by $\det[M] = 0$

$$0 = \begin{bmatrix} (S + v_1 p_0 i q + \frac{\bar{v} v_1 \rho_{10} q^2}{4\alpha_1} + Dq^2) & (-v_1 v_2 \rho_{10} q^2 / 4\alpha_1) & 0 \\ (\Delta v p_0 i q + \frac{\Delta v \bar{v} \rho_{10} q^2}{4\alpha_1}) & (S - \frac{\Delta v v_2 \rho_{10} q^2}{4\alpha_1} + Dq^2 + v_2 p_0 i q) & 0 \\ 0 & 0 & (S - \lambda p_0 i q + k q^2) \end{bmatrix} \tag{2.23}$$

One of the mode $\Rightarrow S = \lambda p_0 i q - k q^2$, which is damped-diffusive oscillatory modes and other two modes are given by

$$0 = \begin{bmatrix} (S + v_1 p_0 i q + q^2 (D + \frac{v_1 \rho_{10} \bar{v}}{4\alpha_1}) & (-v_1 v_2 \rho_{10} q^2 / 4\alpha_1) \\ (\Delta v p_0 i q + \frac{\Delta v \bar{v} \rho_{10} q^2}{4\alpha_1}) & (S + v_2 p_0 i q + q^2 (D - \frac{v_2 \rho_{10} \Delta v}{4\alpha_1}) \end{bmatrix} \tag{2.24}$$

lets define $D_+ = q^2 (D + \frac{v_1 \rho_{10} \bar{v}}{4\alpha_1})$ and $D_- = q^2 (D - \frac{v_2 \rho_{10} \Delta v}{4\alpha_1})$ Hence we have two solutions for S, $\mathscr{R}e(S) > 0$ (mode is unstable) and if $\mathscr{R}e(S) < 0$ (then it is stable)

$$(S + v_1 p_0 i q + q^2 D_+)(S + v_2 p_0 i q + q^2 D_-) + \frac{v_1 v_2 \rho_{10} \Delta v p_0 i q^3}{4\alpha_1} + \frac{\Delta v \bar{v} v_1 v_2 \rho_{10}^2 q^4}{(4\alpha_1)^2} = 0 \tag{2.25}$$

$$2S_\pm = -[(v_1 p_0 i q + D_+ q^2) + (v_2 p_0 i q + D_- q^2)] \pm [(v_1 p_0 i q + D_+ q^2) - (v_2 p_0 i q + D_- q^2)] \tag{2.26}$$

2.6 Discussion

In this chapter, we have studied the binary mixture of polar self-propelled particles with variable speed. The speed of the particle depends on its neighbours, it is maximum in well-aligned region and almost zero in random disordered region. Dependence of local speed on local orientation is controlled by a variable speed parameter γ. The model is motivated with experiments on a fish school where the speed of individual fish depends on its neighbours. We mix the two different types of particles with two different γ values. Where γ_1 is fixed to 1 and another γ_2 is varied from 0 to 8. For $\gamma = 0$, model reduces to constant speed model. Steady state behavior of the system is studied for the different combination of (γ_2, η). For all set of γ's system shows a transition from disordered state to ordered state. We find four different phases: (i) ordered phase separated (OPS) when noise is small and the difference in two γ's is large. In this phase starting from random mixed phase both types of particle phase separate and moves in different clusters. (ii) ordered mixed phase (OM), when the difference in γ is small then all the particles move in well-ordered cluster but in a single cluster both types of particles are present, (iii) disorder mixed phase (DMP), when η is large and difference in two γ is small then both orientation and density order parameter is small and both types of particles remain in mixed phase and have random orientation. (iv) disorder phase segregated (DPS), when noise is large (disorder state) hence for larger γ_2 second type of particles form static clusters with completely random orientation and which acts like nucleation site for first type of more mobile particles. Which leads to a characteristic cluster size for first type particles.

Hence this study shows the appearance of different phases in a binary active mixture of SPP's with variable speed. The variable speed parameter introduced here can be thought of as characteristic of particle species. Hence this study gives insight to phase separation in different particle types, which can be one of the possible reason: why always *same species flock together*? Our current study and model introduced in [Mishra et al. (2012)] motivate

us to look a new approach to understand the variable speed, where the speed of the particle depends on local polarisation. Which is different from the recent variable speed models for active Brownian particles (ABPs) [Fily & Marchetti (2012)], where speed varies with local density.

This chapter is limited to steady state behaviour, it is also interesting to study the ordering kinetics [Bray (1994)] of two types of particles in such mixture.